Diffusion Length Measurements in p-HgCdTe Using Laser Beam Induced Current

D.A. REDFERN,[1,2] J.A. THOMAS,[1] C.A. MUSCA,[1] J.M. DELL,[1] and L. FARAONE[1]

1.—The University of Western Australia, Department of Electrical and Electronic Engineering, Nedlands, 6907, Australia. 2.—e-mail: redfe-da@ee.uwa.edu.au

The minority carrier diffusion length in p-HgCdTe is a key indicator of material quality and gives an indication of n-on-p diode performance when the zero bias resistance is diffusion limited. We present results of a temperature dependent study of diffusion length in p-HgCdTe using laser beam induced current (LBIC). Carriers are collected by a p-n junction formed using standard diode junction formation conditions, and thus not necessarily extending to the substrate. Two-dimensional modeling is used to examine the validity of results obtained using this geometry, as compared to the more standard diffusion length test structure geometries, which are harder to fabricate. The temperature dependence of the diffusion length can be compared with theoretical models to determine the dominant recombination mechanisms.

Key words: Laser beam induced current (LBIC), diffusion length

INTRODUCTION

In situations where the dynamic resistance of HgCdTe photodiodes is diffusion limited, knowledge of the carrier diffusion length can be used to directly calculate the diode resistance.[1] In such situations, long diffusion lengths lead to small dark currents and large diode resistances. Hence, the diffusion length is a key parameter indicating material quality and performance of resulting devices. In this work we present the results of a study of the temperature dependence of diffusion length in a variety of HgCdTe samples, measured using a laser beam induced current (LBIC) technique.

The dimensions of detectors in 2D focal plane arrays have gradually been reduced. When the dimensions of devices are comparable to the diffusion length, the lateral diffusion of carriers to the junction periphery cannot be neglected. This lateral collection leads to an increase of the effective optically sensitive area, allowing the junction area to be reduced, and thus improving device performance.[2] The diffusion length is also an important parameter when considering crosstalk between individual detectors in an array. For analysis of crosstalk and optical area for diode applications, it is advantageous to be able to perform diffusion length measurements on devices fabricated using the standard junction formation process. Traditionally, LBIC and the related electron beam induced current (EBIC) techniques for extracting diffusion lengths require that test structures with special geometries be formed, often requiring the p-n junction to extend perpendicularly the entire distance to the substrate.[3,4] While such geometries produce simple and reliable results, the necessary fabrication process may involve extremes (such as high ion implantation power, or long reactive ion etching, or ion milling duration) which are clearly undesirable and may alter the material properties. In this work we propose to perform the measurements on devices fabricated using standard planar n-on-p diode junction formation conditions, where the n-type region does not generally extend to the substrate. Applications include on-chip test structures formed alongside diodes

(Received November 25, 2000; accepted February 27, 2001)

and fabricated using the same junction formation step.

LBIC has been used previously as a qualitative non-destructive characterization technique, and requires only two remote ohmic contacts to characterize an entire array. A focused low-power laser in a scanning laser microscope is used to generate localized electron-hole pairs. If the region of generation is within a few minority carrier diffusion lengths of a junction, carriers diffusing to the junction will be separated, leading to a lateral photovoltage and an associated current through the remote contacts.[5] Figure 1 shows the LBIC experimental setup and typical induced current profile as the laser is scanned across the device. Note the width, length, and depth of the n-region, which will be referred to in later sections.

The decay of the induced current as the laser is scanned adjacent to the outside edge of the junction is related to the diffusion length in the p-region. However, a number of factors can contribute to discrepancies between the characteristic length, L, extracted by fitting a simple exponential to the LBIC profile, and the true bulk diffusion length, L_p. In the next section, 2D modeling of the LBIC profiles and characteristic length extraction are presented in order to examine the validity of using this geometry, by examining the L/L_p ratio for different combinations of parameters. If we are interested in quantitatively examining material properties using diffusion length measurements, L/L_p is required to be close to 1.0.

Later, a summary of the relevant theory and the experimental setup are outlined, and then results obtained from various samples of p-HgCdTe are presented.

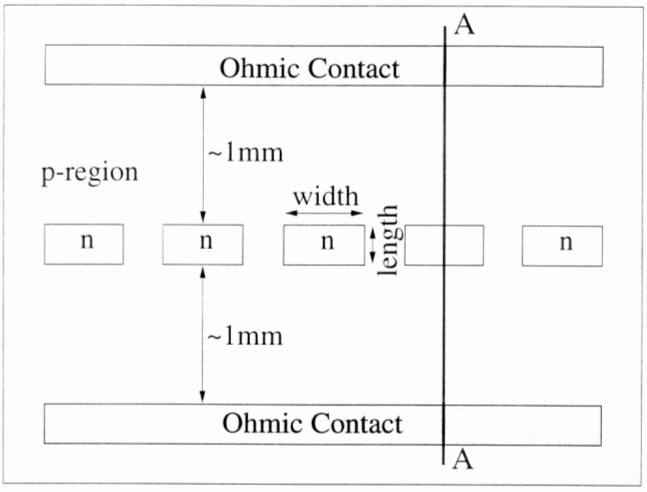

a

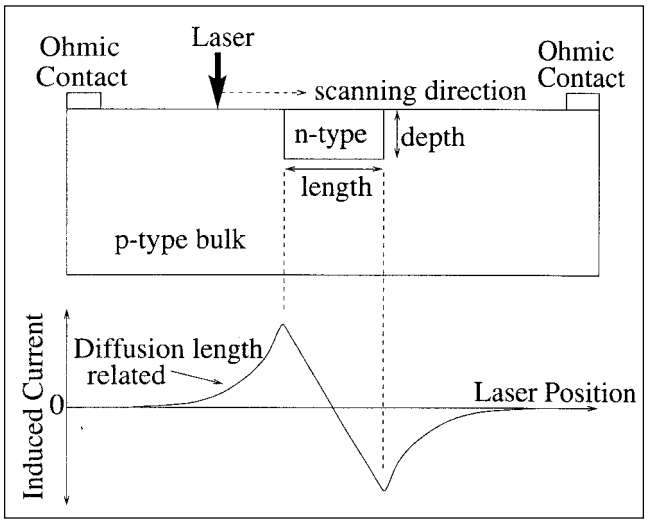

b

Fig. 1. (a) Plan view layout of the samples along with, (b) cross section taken along AA, and the corresponding LBIC profile showing the typical bipolar nature of the signal.

MODELED LBIC

This section presents results of 2D modeling of LBIC in the geometry shown in Fig. 1. The focus of this section is to answer the question of whether the characteristic length obtained by fitting a simple exponential to a part of the LBIC profile is a good representation of the actual bulk diffusion length. The finite dimensions of the n-region and the presence of significant surface recombination can lead to discrepancies between characteristic lengths and diffusion lengths. These factors will be examined, and ways to lessen their effects will be discussed.

Modeling in this section has been performed using a commercial finite element semiconductor modeling package,[6] in combination with a specialized LBIC modeling package adapted from Refs. 7–9 and incorporated into MATLAB using a finite difference scheme. In turn, we discuss the effects of finite device width, depth, and length, as defined in Fig. 1. This is initially done assuming negligible surface recombination, and

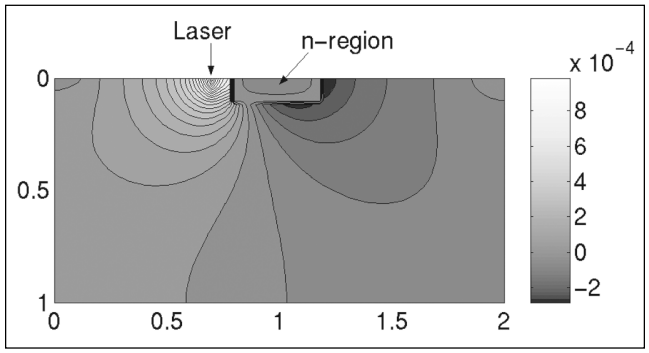

a

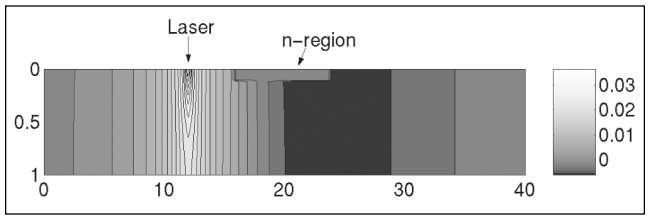

b

Fig. 2. Spatial distribution of excess electron concentration in the device. (a) $L_p = 0.2$, depth = 0.1, length = 0.4, S = 0, $L/L_p = 0.88$. (b) $L_p = 2.0$, depth = 0.1, length = 4.0, S = 0, $L/L_p = 1.0$.

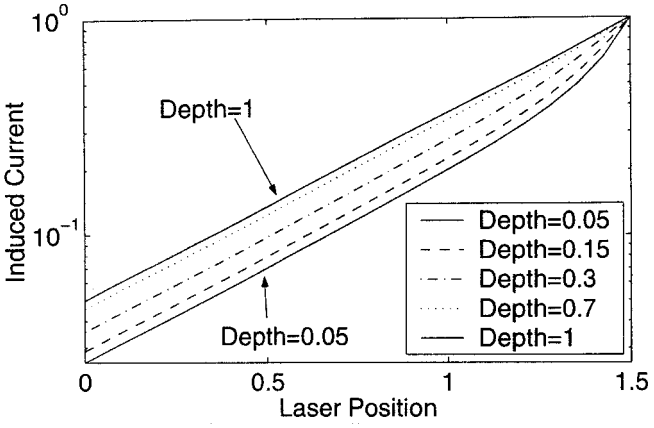

Fig. 3. Induced current decay from the edge of the junction (located at position 1.5) for several junction depths.

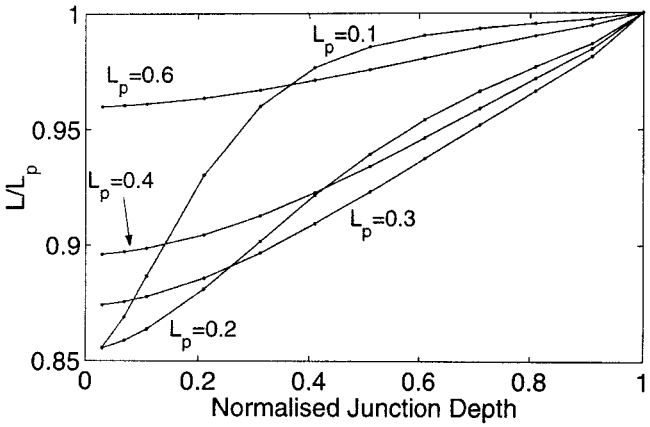

Fig. 4. The ratio of the extracted characteristic length, L, to bulk diffusion length, L_p, for a scaled device length of 0.32 and a variety of bulk diffusion lengths.

then, finally, we introduce surface recombination velocity to examine the effect of non-ideal passivation. There is an inherent relationship between device depth and device length, but we shall first examine device depth for a given device length, and then discuss their interdependence in the device length section.

The results of all modeling are presented in a normalized format, in which all geometrical dimensions and all diffusion lengths are scaled by the sample thickness. This is particularly useful when we consider samples fabricated on HgCdTe epilayers. For example, if the epilayer thickness is 15 μm, then a normalized diffusion length of $L_p = 1.5$ would correspond to an actual diffusion length of 22.5 μm, and a normalized junction depth of 0.1 would represent a 1.5 μm deep junction. Other parameters subject to this scaling are the extracted characteristic length, L, and the device length. Surface recombination is normalized to both the sample thickness and carrier concentration as outlined in Ref. 10. This normalized format allows us to readily model a wide range of device dimensions in a uniform manner.

Experimental measurements were performed using a laser with a 1.047 μm wavelength, and so the generation of photocarriers in the modeling is assumed to be correspondingly close to the surface.

Device Width

In order that a single LBIC line profile can be used in the characteristic length extraction process, the width of the n-region is required to be much larger than the diffusion length. This is important for the validity of the 2D modeling as well as ensuring that carriers will recombine before they have a chance to diffuse around the lateral edges of the device. Wide devices are easily fabricated and so we shall assume that LBIC line profiles are taken through the middle of devices much wider than the diffusion length, such as section AA in Fig. 1a, and hence 2D modeling accurately represents the physical situation.

Device Depth

Characteristic lengths obtained from LBIC profiles of devices whose n-region does not extend all the way to the substrate, such as that shown in Fig. 1, can often give a misleading representation of the diffusion length. Unless the junction is infinitely deep, the movement of carriers can no longer be considered to be one dimensional with respect to the contacts.

Obviously when diffusion lengths are much smaller than the junction depth, the junction appears infinitely deep. This means that the measured characteristic length is the diffusion length for very small diffusion lengths. However, this is no consequence for most practical instances involving HgCdTe since junction depths are of the order of 1–2 μm, and diffusion lengths are usually much larger.

It is quite reasonable to expect carriers generated away from the junction to be able to diffuse under an n-region of finite depth, before they are swept across the junction to take part in setting up the LBIC signal. On average they are diffusing slightly further than the shortest distance to the junction, and thus it could be expected that the measured characteristic lengths are somewhat smaller than the true diffusion lengths. This is the situation portrayed in Fig. 2a, which shows the steady state excess electron distribution in a sample with a diffusion length of 0.2 of the sample thickness. Clearly this distribution of excess carriers implies that some of the carriers diffuse under the n-region and this accounts for the extracted characteristic length being only 0.88 of the diffusion length.

However, most HgCdTe devices are formed on epilayers and the semiconductor-substrate interface (assumed to be perfectly insulating) constrains the carriers to the thin epilayer. This can have a drastic effect on the LBIC diffusion length measurements. If the diffusion length is on the order of, or larger than, the total epilayer thickness, the excess carriers build up between the surface and semiconductor-substrate interface. Figure 2b shows the excess electron distribution for a situation where the diffusion length is twice the epilayer thickness. The characteristic length

extracted from the LBIC associated with this example was found to be equal to the diffusion length, hence the ratio $L/L_p = 1.0$. Note that for positions slightly away from the laser illumination the excess carrier distribution is almost uniform from the surface to the semiconductor-substrate interface, meaning that the diffusion of carriers is effectively one dimensional. Thus, provided the laser is focused onto a spot far enough from the junction to avoid the initial portion of the decay in LBIC profile, the characteristic length will be the diffusion length. This is also seen in Fig. 3 where the slope of the LBIC profile, when shown on a log scale, is independent of junction depth for positions not close to the junction edge (located at position 1.5 in Fig. 3). For a scaled depth of 1.0 the decay is purely exponential, while the initial part of the decay is more rapid for the shallower junctions, reflecting the effect of the carriers being able to diffuse under the n-region. Note that in this case the more rapid decay is not caused by surface effects.

Figure 4 shows the ratio of extracted characteristic length, L, to diffusion length, L_p, as a function of junction depth for a scaled device length of 0.32 and a variety of diffusion lengths. For each diffusion length the L/L_p ratio increases monotonically as the junction depth increases. For this particular device length the measured characteristic length deviates from the true diffusion length for all diffusion lengths shown, at all scaled depths less than 1.

The general trend for increasing diffusion length, larger than approximately a quarter of the total epilayer thickness, is that the L/L_p ratio increases. Thus we are approaching the one dimensional situation of Fig. 2b and characteristic lengths are approaching the bulk diffusion length.

The anomalous curves associated with $L_p < 0.3$ show that when the diffusion lengths are much shorter than the junction depth the n-region begins to appear very deep, and the L/L_p increases. Obviously, this effect is more pronounced for very small diffusion lengths.

Hence, diffusion lengths much smaller than the epilayer thickness, and diffusion lengths on the order of, or larger than, the sample thickness, can both give large L/L_p ratios. It is mainly intermediate diffusion lengths at which the characteristic lengths deviate significantly from the diffusion length.

While Fig. 4 has been calculated for one particular device length, and the situation is highly dependent on device length, the general trends still hold. It will be shown that for most practical device lengths if L_p is long enough or short enough L/L_p approaches 1.0 for any junction depth.

Device Length

The device length examined in the previous section is very small in practical terms, representing a device length of just over 6 μm in a 20 μm epilayer for example. In this section we examine how the situation changes for device lengths that are more practical.

Figure 5 shows calculated L/L_p values as a function of device length for a few diffusion lengths and junction depths. Undoubtedly, there is a complex relationship between junction depth, device length and diffusion length, and the resulting value of the ratio L/L_p, however, a few generalizations can be made.

When the diffusion length is significantly smaller than the sample thickness, such as the $L_p = 0.2$ of Fig. 5a, very long device lengths may be required to

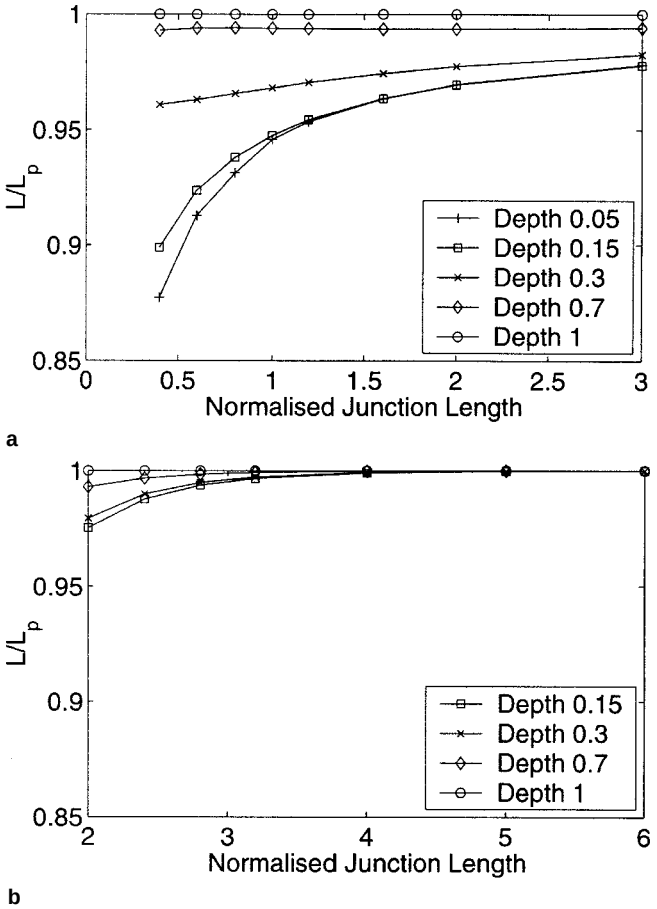

Fig. 5. Effect of device length on extracted characteristic length.(a): $L_p = 0.2$, $S = 0$. (b) $L_p = 1.0$, $S = 0$.

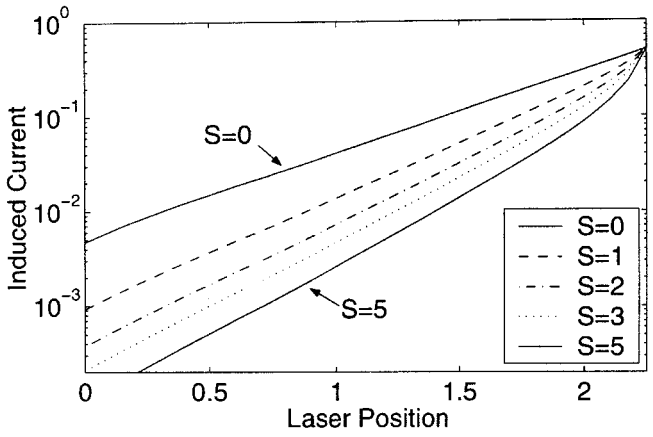

Fig. 6. The effect of surface recombination on the decay of induced current away from the device edge (located on the right edge of the figure).

Table. I. Sample Data for p-type HgCdTe Used in This Study

Sample ID	Source	x	Dopant	p (cm^{-3})	μ_h ($cm^2V^{-1}s^{-1}$)	Length (μm)	Thickness (μm)
27170*	Fermionics	0.22	Vacancy	7.1×10^{15}	695	50–200	19
PACE	Rockwell	0.31	Vacancy	2.0×10^{16}	400	200	13
95197	Fermionics	0.27	Vacancy	9.0×10^{16}	360	400	19
30173	Fermionics	0.3	Vacancy	5.8×10^{15}	420	200	~18
95189	Fermionics	0.31	Au	1.6×10^{16}	400	200	~18

* Passivation with ZnS

ensure L/L_p is close to 1, specially for very shallow junctions. Conversely, considering smaller device lengths, L/L_p may still be quite large (above 0.9) for device lengths down to about the order of L_p.

For larger diffusion lengths, on the order of or larger than the sample thickness (see for example Fig. 5b in which L_p=1.0), device lengths larger than 3 or 4 times the epilayer thickness would ensure L/L_p very close to 1.0. Thus we could expect characteristic lengths extracted from LBIC measurements on a 80 μm long device fabricated on a 20 μm epilayer to accurately represent the diffusion length provided the diffusion length is around 20 μm or larger. However, when device lengths are decreased below approximately 1, such that device length is smaller than L_p, the L/L_p ratio decreases significantly (not shown here).

Note that the required device lengths for high L/L_p ratios will be smaller when thinner epilayers are used, since this corresponds to a larger scaled diffusion length and a larger scaled device length.

Surface Recombination Velocity

In this section we introduce surface recombination into the modeling. Surface recombination typically results in a more rapid transient decay of the excess minority carriers. In a steady state regime, such as LBIC, this manifests itself as a spatial profile that initially decays more rapidly than exponential as the laser is scanned away from the edge of the junction (see Fig. 6). Further away from the junction the decay returns to exponential, however, as can clearly be seen by the different slopes in Fig. 6, the characteristic decay length depends on the surface recombination velocity. Note also how the profiles decay more rapidly than exponential when the laser is close to the n-region, in a similar way to the effect of variation of junction depth shown in Fig. 3. However, the data for Fig. 6 was calculated for an n-region extended all the way to the semiconductor-substrate interface. The more rapid decay close to the edge of the n-region in Fig. 6 is purely due to the surface recombination.

Figure 7 shows calculated values of L/L_p as a function of normalized surface recombination velocity for a variety of junction depths and diffusion lengths.

Surface recombination velocities and bulk diffusion lengths can be extracted[3,4] provided the more rapid decay close to the junction is entirely due to surface effects. When significant surface recombination exists on a sample in which the junction depth is shallow, the more rapid initial decay will be due to a combination of surface and geometrical effects, and it is much more difficult to separate these effects unless other assumptions are made.

Surface recombination can be avoided or reduced by appropriate passivation of the sample. Provided the initial part of the decay signal is ignored in the fitting procedure, a characteristic length can be obtained, taking into account bulk and surface effects. While this characteristic length is not suitable for use in examining bulk recombination mechanisms, it can represent an effective diffusion length of combined

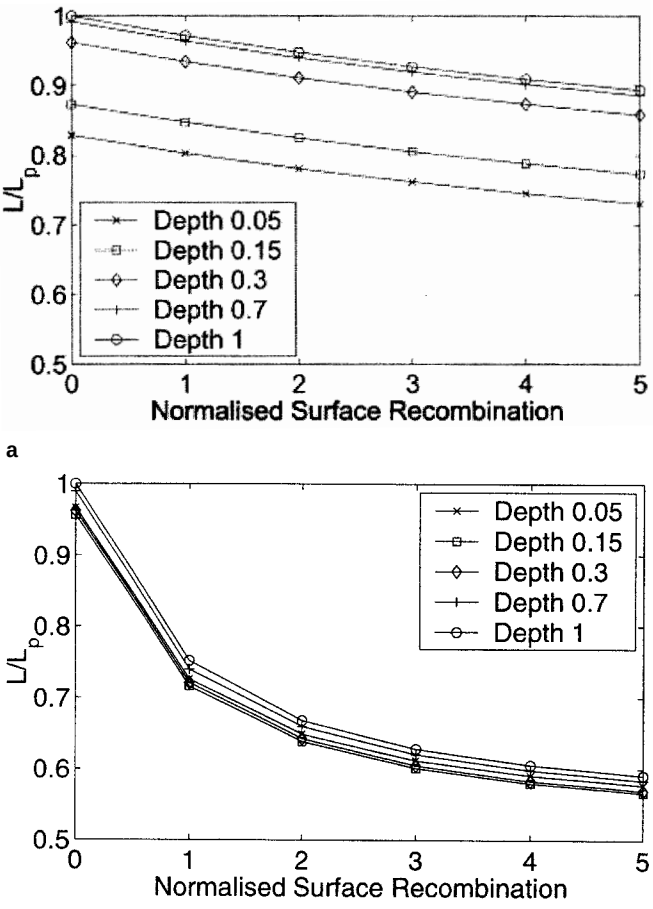

Fig. 7. The effect of surface recombination velocity on the extracted characteristic length.(a): L_p = 0.2, length = 0.4. (b) L_p = 2.0, length = 3.0.

bulk and surface effects if the devices are long enough and diffusion lengths larger than some proportion of the epilayer thickness.

Regardless of the geometry of the device, the characteristic length is still useful in defining the effective optical area of the devices, which is often used in determining the R_0A_{opt} of devices.[11] The optical area is simply the area from which photogenerated carriers are collected from, and, clearly, this will be effected by geometry as well as bulk and surface properties.

THEORY

The bulk diffusion length in the p-type material, Lp, is related to the minority carrier lifetime, τ_p, by the following expression.

$$L_p = \sqrt{D\tau_p} \tag{1}$$

In this equation D is an appropriate diffusion coefficient, most generally the ambipolar diffusion coefficient given by

$$D = \frac{D_e D_h (n+p)}{nD_e + pD_h}$$

D_h and D_e are the diffusion coefficients of holes and electrons, respectively, and are related to the hole and electron mobilities by Einstein's relations,

$$D_h = \frac{kT}{q}\mu_h \text{ and } D_e = \frac{kT}{q}\mu_e$$

In the situation where $p\mu h >> n\mu e$, such as in p-type material at low temperatures, we have $D \approx D_h$ and so Eq. 1 reduces to

$$L_p = \sqrt{D_h\tau_p}$$

For purposes of comparison of the diffusion length data to the theoretical temperature dependence, the well accepted empirical relationship for the temperature dependence of the electron and hole mobility for $0.2 \le x \le 0.6$ and $T > 50$ K is assumed.

$$\mu_e = A\frac{9\times10^8 b}{T^{2a}} \text{ and } \mu_h = \frac{\mu_e}{100}$$

where

$$a = \left(\frac{0.2}{x}\right)^{0.6} \text{ and } b = \left(\frac{0.2}{x}\right)^{7.5}$$

These equations are modified from Ref. 12 by the inclusion of A, a scaling factor chosen so that the mobility at 77 K matches the suppliers value. This accounts for differences in mobilities caused by different doping.

The diffusion length can then be related directly to theoretical expressions for carrier lifetime to determine the dominant recombination mechanisms. The carrier lifetime, τ_p, is a combination of various recombination mechanisms, which are assumed independent.

$$\frac{1}{\tau_p} = \frac{1}{\tau_{SRH}} + \frac{1}{\tau_R} + \frac{1}{\tau_A}$$

τ_{SRH} is the Shockley-Read-Hall recombination lifetime, τ_R is the lifetime of carriers involved in radiative recombination, and τ_A is the Auger recombination lifetime, which is composed of Auger-1 and Auger-7 contributions. The expressions for these mechanisms are listed in the Appendix.

EXPERIMENTAL PROCEDURES

For the experimental part of the study five samples of p-type HgCdTe were chosen with different compositions and doping densities. Full details of the samples are shown in Table I. Sample 27170 was passivated with thermally deposited ZnS, the remaining samples were unpassivated but measured with freshly etched surfaces.

Each sample was thinned using a 0.1% solution of Br in methanol and the epilayer thicknesses determined using Fourier transform infrared (FTIR) spectroscopy. One dimensional arrays of n-on-p planar diode structures were then formed in the layout of Fig. 1a. The junctions were 400 μm wide and of lengths specified in the table, and were formed using

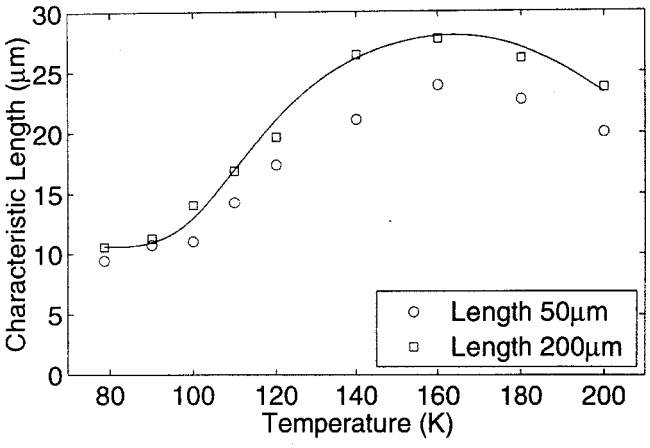

Fig. 8: Sample 27170 (x = 0.22, p = 7.1 × x10^{15} cm^{-3}). Measured characteristic lengths for 50 μm and 200 μm device lengths along with a theoretical fit to the predicted temperature dependence.

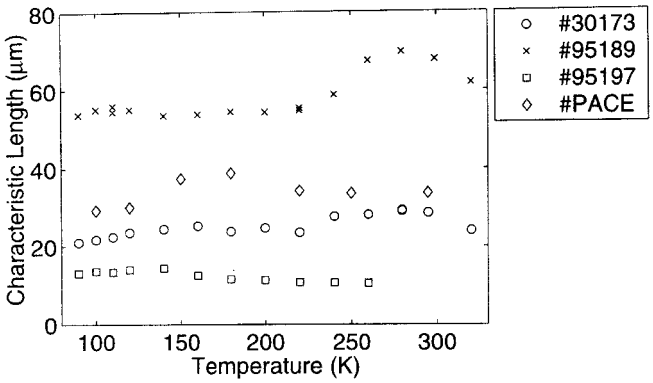

Fig. 9. Temperature dependence of the characteristic decay lengths of the remaining samples.

a reactive ion etching (RIE) plasma junction formation technique.[13] The RIE conditions (0.4 Wcm^{-2}, 2 min., 100 mtorr, H_2:CH_4 ratio of 3:1) have been found to produce a junction depth on the order of 2 μm in p-HgCdTe. Strip contacts to the p-type material were deposited at least 1 mm from the edges of the devices as in Fig. 1a and then LBIC measurements were taken at a number of temperatures. The characteristic length of the LBIC decay was obtained by fitting a simple exponential to the decay of the profile obtained as the laser was scanned away from the junction. The samples had up to eleven devices between the strip contacts, depending on the size of the samples, and the characteristic lengths were averaged over all devices.

RESULTS

Two arrays of devices with different device lengths were fabricated on sample 27170. The ZnS passivation is assumed to be good enough that surface recombination can be ignored, and so the characteristic lengths could represent diffusion lengths provided the geometry is suitable. Figure 8 shows the temperature dependence of these characteristic lengths obtained from the arrays of 50 μm and 200 μm wide devices. Clearly the 50 μm devices had characteristic lengths smaller than those of the 200 μm wide devices over the entire temperature range. If it is assumed that the characteristic lengths obtained from the 200 μm array are the true diffusion lengths, then the ratio L/L_p for the 50 μm devices ranges from about 0.79 to 0.95 with an average over all ratio of 0.86. It is expected that the discrepancies between measurements on the two arrays is due to the geometrical effects of the different length devices, as discussed in the previous sections. However, in consideration of the modeling results, and Fig. 5b in particular, the L/L_p ratio of 0.86 for devices with a scaled length of around 2.5 is very low. A smaller scaled length could account for the discrepancy, meaning that the epilayer might actually be behaving thicker than it really is. This would indicate that factors other than those considered in the modeling could be involved, such as a very slight grading of the p-doping decreasing towards the surface, somewhat impeding the diffusion of minority carriers towards the substrate.

While the measured characteristic decay lengths for the 200 μm long devices are not uniformly larger than the epilayer thickness, they are assumed to be the diffusion length, and a theoretical fit to the temperature dependence of the diffusion length is shown in Fig. 8. Detailed analysis shows that the diffusion length is limited by Auger-7 recombination at temperatures above 160 K and by a combination of the Auger-7 and Shockley-Read-Hall recombination mechanisms at lower temperatures.

Samples other than sample 27170 were unpassivated. The characteristic lengths obtained from these samples can only represent effective diffusion lengths since surface recombination is expected to be a contributor in each case. Figure 9 shows the temperature dependence of the characteristic lengths obtained from the remaining samples. The general trend of diffusion lengths decreasing with increased doping is evident in the vacancy doped samples, with sample 95197 having the shortest characteristic lengths and the highest doping. However, the gold doped sample, with a moderate doping, stands out as easily having the longest characteristic lengths.

CONCLUSIONS

Characteristic decay lengths have been measured as a function of temperature using LBIC on devices formed using standard junction formation conditions used for high performance n-on-p diode fabrication. This geometry is much easier to fabricate than traditional diffusion length test structures because the n-region does not in general extend to the substrate. Additionally, this is the geometry that should be used when calculating the effective optical area of devices, since the geometry, and in particular the junction depth, does have an effect on the collection area.

Two dimensional modeling has been performed to determine whether characteristic lengths measured on these structures reflect the true bulk diffusion length. For the case of zero surface recombination, it was shown that provided the diffusion length and the device length are both long enough, in relation to the sample thickness, then the characteristic length is the same as the diffusion length. When surface recombination is significant the characteristic length can represent an effective diffusion length provided diffusion lengths and device lengths are long enough. However, when surface recombination is significant, it is extremely difficult to extract values for both the surface recombination velocity and bulk diffusion length, unless other assumptions are made.

Using theoretical expressions for carrier recombination mechanisms and an empirical relation for the temperature dependence of mobility, it is possible to compare the measured diffusion lengths with the theoretical temperature dependence, and thus gain knowledge of the mechanisms limiting the diffusion length.

ACKNOWLEDGEMENTS

The authors wish to thank Dr. R. Pal for assistance with the measurements, and Dr. M.H. Rais for fabrication of some of the devices. This work was carried out with the financial support of the Australian Research Council.

REFERENCES

1. A. Rogalski, *Infrared Phys.* 28, 139 (1988).
2. M.B. Reine, A.K. Sood, and T.J. Tredwell, *Semiconductors and Semimetals,* Vol. 18, ed. R.K. Willardson and A.C. Beer (New York: Academic Press, 1981), pp. 238–240.
3. K.L. Luke and L. Cheng, *J. Appl. Phys.* 61, 2282 (1987).
4. V.K.S. Ong, J.C.H. Phang, and D.S.H. Chan, *Solid-State Electron.* 37, 1 (1994).
5. J.T. Wallmark, *Proc. IRE*, 45, 474 (1957).
6. *Medici,* version 1998.4.1 (Fremont, CA: Avant! Corp. and TMA Inc., 1998).

7. W. Fang and K. Ito, *SIAM J. Appl. Math.* 52, 1611 (1992).
8. S. Busenberg, W. Fang, and K. Ito, *SIAM J. Appl. Math.* 53, 187 (1993).
9. W. Fang and K. Ito, *SIAM J. Appl. Math.* 54, 1067 (1994).
10. D.A. Redfern, W. Fang, K. Ito, J.M. Dell, and L. Faraone (unpublished).
11. A.I. D'Souza, P.S. Wijewarnasuriya, R.E. Dewarmes, G. Hilderbrandt, J. Bajaj, D.D. Edwall, J.G. Pasko, and J.M. Arias, *J. Electron. Mater.* 28, 611 (1999).
12. J.P. Rosbeck, R.E. Starr, S.L. Price, and K.J. Riley, *J. Appl. Phys.* 53, 6430 (1982).
13. J.M. Dell, J. Antoszewski, M.H. Rais, C.A. Musca, J.K. White, B.D. Nener, and L. Faraone, *J. Electron. Mater.* 29, 841 (2000).
14. R. Fastow, D. Goren, and Y. Nemirovsky, *J. Appl. Phys.* 68, 3405 (1990).
15. S. Barton, D. Dutton, P. Capper, C.L. Jones, and N. Metcalfe, *J. Electron. Mater.* 21, 1759 (1995).
16. T.N. Casselman and P.E. Petersen, *Solid State Commun.* 33, 615 (1980).
17. T.N. Casselman, *J. Appl. Phys.* 52, 848 (1981).

APPENDIX: RECOMBINATION MECHANISMS

Shockley-Read-Hall recombination lifetime is given by

$$\tau_{SRH} = \frac{\tau_{p0}(n_0 + n_1) + \tau_{n0}(p_0 + p_1)}{n_0 + p_0}$$

where $\tau_{n0} = 1/(\sigma_n N_t)$ and $\tau_{p0} = 1/(\sigma_p N_t)$.[14] In these expressions σ_n and σ_p are the capture cross sections for electrons and holes, and N_t is the Shockley-Read-Hall trap density. n_1 and p_1 are related to N_c, N_v (the effective density of states in the conduction and valence bands, respectively), E_c, E_v, and E_t (the energies of the conduction band edge and valance band edge and the discrete energy of the trap) by the following relationships.

$$n_1 = N_c \exp\left(\frac{(E_c - E_t)}{kT}\right), \text{and } p_1 = N_v \exp\left(\frac{(E_t - E_v)}{kT}\right)$$

Radiative recombination lifetime is given by[15]

$$\tau_R = \frac{n_i^2}{G_r(n_0 + p_0 + n_e)},$$

where n_i is the intrinsic carrier concentration, n_0 and p_0 are the equilibrium electron and hole densities, n_e is the excess carrier density, and G_r is the thermal equilibrium generation rate.

The most predominant Auger recombination mechanisms in HgCdTe are the Auger-1 and Auger-7,[16,17] which have characteristic lifetimes τ_{A1} and τ_{A7}, respectively. The net Auger lifetime is given by

$$\tau_A = \frac{\tau_{A1}\tau_{A7}}{\tau_{A1} + \tau_{A7}}$$

and individual expressions for τ_{A1} and τ_{A7} are as follows.

$$\tau_{A1} = \frac{2\tau_{A1}^{(i)}}{1 + (n_0 / n_i)^2}$$

where $\tau_{A1}^{(i)}$ is the intrinsic Auger-1 lifetime given by

$$\tau_{A1}^{(i)} = 3.8 \times 10^{-18} \in^2 (1+\mu)^{0.5}(1+2\mu) \exp\left(\frac{(1-2\mu)E_g}{(1+\mu)kT}\right)\left(\frac{m_0}{m_e^*}\right) |F_1F_2|^{-2} \left(\frac{E_g}{kT}\right)^{1.5}$$

where $\mu = \frac{m_e^*}{m_h^*}$, $\in$ is the optical dielectric constant, E_g is the bandgap energy, k is Boltzmann's constant, T is the temperature, m_0 is the electron rest mass, and F_1F_2 is the overlap integral.

$$\tau_{A7} = \frac{2\tau_{A7}^{(i)}}{1 + (p_0 / n_i)^2}$$

where the intrinsic Auger-7 lifetime can be obtained via the ratio of intrinsic Auger-7 to intrinsic Auger-1 lifetime,[16]

$$\gamma = \frac{\tau_{A7}^{(i)}}{\tau_{A1}^{(i)}} \approx 2\frac{m_e^*(E_{th})(1 - \frac{5E_{th}}{4kT})}{m_{eo}^*(1 - \frac{3E_{th}}{2kT})}$$